Progress In Electromagnetics Research, PIER 35, 271–286, 2002

PROPAGATION OF ELECTROMAGNETIC WAVES IN A SLAB WITH NEGATIVE PERMITTIVITY AND NEGATIVE PERMEABILITY

Y. Zhang, T. M. Grzegorczyk, and J. A. Kong

Research Laboratory of Electronics
Massachusetts Institute of Technology
Cambridge, MA 02139, USA

Abstract—In this paper, we study the electromagnetic fields propagating through a slab which permittivity and permeability are simultaneously negative. We show that symmetry properties of the wave solution remove all ambiguity in the choice of the sign of the wave numbers inside the slab. Upon developing the Green's functions in terms of plane waves, growing "evanescent" waves in the direction of power flow are shown to exist inside the slab. As an illustration, the perfect imaging property of a slab where $\epsilon_1 = -\epsilon_0$ and $\mu_1 = -\mu_0$ is verified.

1. INTRODUCTION

Until recently, materials possessing both negative permittivity and permeability simultaneously have been merely a theoretical concept, without any prospect of an impact on the technological world. After the first theoretical consideration in 1968 [1], there has been little effort to better understand the electromagnetic behaviors of these materials for almost three decades. It is only recently, in 1996 for the permittivities [2], and in 1999 for the permeabilities [3], that the possibility of realizing plasma-like structures in the GHz band has been demonstrated experimentally. These contributions have then been naturally followed in year 2000 by the first realization of a material with simultaneously negative permittivities and permeabilities in the GHz band [4].

After [1], one of the very first theoretical contribution was offered in [5], where the focusing property of a loss-less non-dispersive slab made of a material with both negative permittivity and permeability has been demonstrated. In this contribution, the author not only discussed the question of propagating waves but also of evanescent waves, showing that the overall transmission process through both interfaces of the slab results in an increase in their amplitude. The ability to focus both propagating and evanescent waves was thus appropriately used to justify the denomination of a "perfect lens". However, despite these already involved theoretical considerations, the main demonstration in [5] was based on a ray-optics approximation and consequently, a more rigorous approach was still lacking in literature.

The present paper is aimed at providing such a detailed analysis. The approach we have chosen first expresses the electromagnetic fields inside and outside a loss-less non-dispersive slab with arbitrary permittivity and permeability by using the layered Green's function in plane wave expansion for an excitation current source. Then the coefficients in the Green's functions' kernels are solved by matching the boundary conditions for tangential electric and magnetic fields. Upon carefully carrying the algebra of the problem, it is shown that the mathematical expressions governing the fields inside the dielectric slab are symmetric with respect to both the total wavenumber (k_1 in this paper) and the longitudinal wavenumber (k_{1z} in this paper). Consequently, the delicate issue of having to choose a sign for k_{1z} is avoided in this way. Finally, for the sake of validation with some recent properties discussed in the literature, we also study the propagation of waves through a slab of a material with both negative permittivity and permeability, $\epsilon_1 = -\epsilon_0$, $\mu_1 = -\mu_0$ (ϵ_1 and μ_1 being the constitutive parameters of the slab). It is then rigorously shown that, for this

special case, if the current source is located from the first dielectric interface at a distance smaller than the slab thickness, an identical field distribution ("image") is obtained inside the slab and a second one at the exit of the slab.

2. FORMULATION OF THE PROBLEM

Consider a current source $\overline{J}$ situated at a distance h above a homogeneous slab of thickness d, with arbitrary permittivity and permeability (ϵ_1, μ_1), as depicted in Fig. 1. The regions $z > 0$ and $z < -d$ are free-space (ϵ_0, μ_0). In order to study the electromagnetic waves and the Poynting power emanating from $\overline{J}$ and propagating through the slab, the layered Green's function formulation is employed.

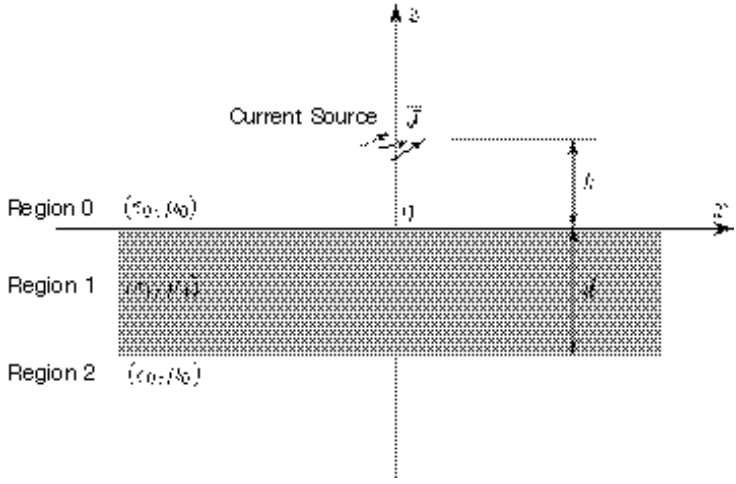

Figure 1. A current source $\overline{J}$ placed above a slab by both negative permittivity and negative permeability.

2.1. Layered Green's Function and Boundary Conditions

The mathematical development of the problem starts by constructing the layered Green's functions, $\overline{\overline{G}}_{n0}$ (where n denoting the region of the observation and 0 representing the region of the source), in a classical plane wave expansion. The main advantage of proceeding this way in our case is the possibility of using these Green's functions for arbitrarily distributed current sources. In the situation of Fig. 1, the layered Green's functions are written as [6, page 853]:

1. In region 0, above the slab ($0 < z < z'$):

$$\begin{aligned}
&\overline{\overline{G}}_{00}(\overline{r},\overline{r}') \\
&= \frac{i}{8\pi^2}\iint \mathrm{d}k_x \mathrm{d}k_y \frac{1}{k_{0z}} \Big\{ \left[\hat{e}(-k_{0z})e^{i\overline{K}\cdot\overline{r}} + R^{TE}\hat{e}(k_{0z})e^{i\overline{k}\cdot\overline{r}}\right] \hat{e}(-k_{0z})e^{-i\overline{K}\cdot\overline{r}'} \\
&\quad + \left[\hat{h}(-k_{0z})e^{i\overline{K}\cdot\overline{r}} + R^{TM}\hat{h}(k_{0z})e^{i\overline{k}\cdot\overline{r}}\right] \hat{h}(-k_{0z})e^{-i\overline{K}\cdot\overline{r}'} \Big\} \qquad (1)
\end{aligned}$$

2. In region 1, inside the slab ($-d < z < 0$):

$$\begin{aligned}
&\overline{\overline{G}}_{10}(\overline{r},\overline{r}') \\
&= \frac{i}{8\pi^2}\iint \mathrm{d}k_x \mathrm{d}k_y \frac{1}{k_{0z}} \Big\{ \left[B\hat{e}_1(-k_{1z})e^{i\overline{K}_1\cdot\overline{r}} + A\hat{e}_1(k_{1z})e^{i\overline{k}_1\cdot\overline{r}}\right] \hat{e}(-k_{0z})e^{-i\overline{K}\cdot\overline{r}'} \\
&\quad + \left[D\hat{h}_1(-k_{1z})e^{i\overline{K}_1\cdot\overline{r}} + C\hat{h}_1(k_{1z})e^{i\overline{k}_1\cdot\overline{r}}\right] \hat{h}(-k_{0z})e^{-i\overline{K}\cdot\overline{r}'} \Big\} \qquad (2)
\end{aligned}$$

3. In region 2, below the slab ($z < -d$):

$$\begin{aligned}
\overline{\overline{G}}_{20}(\overline{r},\overline{r}') \;=\; & \frac{i}{8\pi^2}\iint \mathrm{d}k_x \mathrm{d}k_y \frac{1}{k_{0z}} \Big\{ T^{TE}\hat{e}(-k_{0z})e^{i\overline{K}\cdot\overline{r}}\hat{e}(-k_{0z})e^{-i\overline{K}\cdot\overline{r}'} \\
& + \left[T^{TM}\hat{h}(-k_{0z})e^{i\overline{K}\cdot\overline{r}}\right] \hat{h}(-k_{0z})e^{-i\overline{K}\cdot\overline{r}'} \Big\} \qquad (3)
\end{aligned}$$

where TE and TM are the classical two polarization states, R and T are the reflection and transmission coefficients, respectively, and A, B, C, D are four constants to be determined from the boundary conditions. Vectors $\hat{e}$ and $\hat{h}$ are the polarization vectors outside the slab whereas $\hat{e}_1$ and $\hat{h}_1$ are inside the slab, respectively, defined by:

$$\hat{e}(\pm k_{0z}) = \frac{\hat{x}k_y - \hat{y}k_x}{(\hat{x}k_x + \hat{y}k_y)} \qquad (4)$$

$$\hat{h}(\pm k_{0z}) = \frac{\mp k_{0z}}{k\sqrt{k_x^2 + k_y^2}}(\hat{x}k_x + \hat{y}k_y) + \hat{z}\frac{\sqrt{k_x^2 + k_y^2}}{k} \qquad (5)$$

$$\hat{e}_1(\pm k_{0z}) = \frac{\hat{x}k_y - \hat{y}k_x}{\sqrt{k_x^2 + k_y^2}} \qquad (6)$$

$$\hat{h}_1(\pm k_{1z}) = \frac{\mp k_{1z}}{k_1\sqrt{k_x^2 + k_y^2}}(\hat{x}k_x + \hat{y}k_y) + \hat{z}\frac{\sqrt{k_x^2 + k_y^2}}{k_1} \qquad (7)$$

and the wave vectors $\overline{k}$ and $\overline{K}$ are defined by:

$$\overline{k} = \hat{x}k_x + \hat{y}k_y + \hat{z}k_{0z} \qquad (8)$$

$$\overline{K} = \hat{x}k_x + \hat{y}k_y - \hat{z}k_{0z} \qquad (9)$$

for regions 0 and 2, and

$$\overline{k}_1 = \hat{x}k_x + \hat{y}k_y + \hat{z}k_{1z} \tag{10}$$

$$\overline{K}_1 = \hat{x}k_x + \hat{y}k_y - \hat{z}k_{1z} \tag{11}$$

for region 1.

The integrations in Eqs. (1)–(3) to be conducted in terms of k_x and k_y are over entire real space (from $-\infty$ to ∞). Note that the horizontal components of the wave vectors, k_x and k_y, are the same in all the regions due to phase matching, whereas the vertical components k_{0z} and k_{1z} are, in general, discontinuous. The various coefficients, namely the reflection ($R^{TE,TM}$) and transmission ($T^{TE,TM}$) coefficients as well as A, B, C, D, are determined by a proper application of the boundary conditions discussed in the following.

Given a current distribution $\overline{J}$, the electric fields in region n, where $n \in \{0, 1, 2\}$, are expressed as

$$\overline{E}_n(\overline{r}) = i\omega\mu_0 \int \overline{\overline{G}}_{n0}(\overline{r}, \overline{r}') \cdot \overline{J}(\overline{r}') d\overline{r}' \tag{12}$$

By satisfying the boundary conditions for tangential electric and magnetic fields at $z = 0$ and $z = -d$, we obtain the system of equations shown in Appendix A.1 for the coefficients R^{TE}, R^{TM}, R^{TE}, R^{TM}, A, B, C, and D. The solutions from these equations are as follows:

$$R^{TE} = \frac{1 - e^{2ik_{1z}d}}{1 + R_{01}^{TE} R_{10}^{TE} e^{i2k_{1z}d}} R_{01}^{TE} \tag{13}$$

$$T^{TE} = \frac{4e^{i(k_{1z} - k_{0z})d}}{\left(1 + p_{01}^{TE}\right)\left(1 + p_{10}^{TE}\right)\left(1 + R_{01}^{TE} R_{10}^{TE} e^{i2k_{1z}d}\right)} \tag{14}$$

$$R^{TM} = \frac{1 - e^{2ik_{1z}d}}{1 + R_{01}^{TM} R_{10}^{TM} e^{i2k_{1z}d}} R_{01}^{TM} \tag{15}$$

$$T^{TM} = \frac{4e^{i(k_{1z} - k_{0z})d}}{\left(1 + p_{01}^{TM}\right)\left(1 + p_{10}^{TM}\right)\left(1 + R_{01}^{TM} R_{10}^{TM} e^{i2k_{1z}d}\right)} \tag{16}$$

$$A = \frac{1 - p_{10}^{TE}}{2} \left(\frac{1 + R_{01}^{TE} R_{10}^{TE}}{1 + R_{01}^{TE} R_{10}^{TE} e^{i2k_{1z}d}} \right) e^{2ik_{1z}d} \tag{17}$$

$$B = \frac{1 + R_{01}^{TE}}{1 + R_{01}^{TE} R_{10}^{TE} e^{i2k_{1z}d}} \tag{18}$$

$$C = \frac{\mu_1 k}{\mu_0 k_1} \frac{2R_{10}^{TM}}{\left(1 + p_{01}^{TM}\right)\left(1 + R_{01}^{TM} R_{10}^{TM} e^{i2k_{1z}d}\right)} e^{i2k_{1z}d} \tag{19}$$

$$D = \frac{\mu_1 k}{\mu_0 k_1} \frac{2}{\left(1 + p_{01}^{TM}\right)\left(1 + R_{01}^{TM} R_{10}^{TM} e^{i2k_{1z}d}\right)} \tag{20}$$

Appendix A.2 lists the parameter $p_{01}^{TE,TM}$ and the Fresnel reflection coefficient $R_{01}^{TE,TM}$ on the $z = 0$ surface, as well as $p_{10}^{TE,TM}$ and $R_{10}^{TE,TM}$ on the $z = -d$ surface.

2.2. Symmetry Properties of the Green's Functions

After a close examination of Eqs. (13)–(20), the following symmetry properties can be verified:

$$R^{TE,TM}(-k_{1z}) = R^{TE,TM}(k_{1z}) \tag{21}$$
$$T^{TE,TM}(-k_{1z}) = T^{TE,TM}(k_{1z}) \tag{22}$$
$$A(\mp k_{1z}) = B(\pm k_{1z}) \tag{23}$$
$$C(\mp k_{1z}) = D(\pm k_{1z}) \tag{24}$$

so that we immediately conclude that the Green's functions $\overline{\overline{G}}_{00}$ and $\overline{\overline{G}}_{20}$, and the fields in regions 0 and 2, are invariant with respect to the sign of k_{1z}, i.e.,

$$\overline{\overline{G}}_{00,20}(-k_{1z}) = \overline{\overline{G}}_{00,20}(k_{1z}) \tag{25}$$
$$\overline{E}_{0,2}(-k_{1z}) = \overline{E}_{0,2}(k_{1z}) \tag{26}$$
$$\overline{H}_{0,2}(-k_{1z}) = \overline{H}_{0,2}(k_{1z}) \tag{27}$$

In addition, by using the symmetry properties of Eqs. (23) and (24), we obtain the following relations for the summation terms in Eq. (2):

$$\begin{aligned} &B(-k_{1z})\,\hat{e}_1(k_{1z}) e^{i\overline{k}_1\cdot\overline{r}} + A(-k_{1z})\hat{e}_1(-k_{1z}) e^{i\overline{K}_1\cdot\overline{r}} \\ &\qquad = A(k_{1z})\hat{e}_1(k_{1z}) e^{i\overline{k}_1\cdot\overline{r}} + B(k_{1z})\hat{e}_1(-k_{1z}) e^{i\overline{K}_1\cdot\overline{r}} \end{aligned} \tag{28}$$

$$\begin{aligned} &C(-k_{1z})\,\hat{h}_1(k_{1z}) e^{i\overline{k}_1\cdot\overline{r}} + D(-k_{1z})\hat{h}_1(-k_{1z}) e^{i\overline{K}_1\cdot\overline{r}} \\ &\qquad = C(k_{1z})\hat{h}_1(k_{1z}) e^{i\overline{k}_1\cdot\overline{r}} + D(k_{1z})\hat{h}_1(-k_{1z}) e^{i\overline{K}_1\cdot\overline{r}} \end{aligned} \tag{29}$$

These relations imply that, in region 1, the Green's function, as well as the fields, are also invariant with respect to the sign of k_{1z}, i.e.,

$$\overline{\overline{G}}_{10}(-k_{1z}) = \overline{\overline{G}}_{10}(k_{1z}) \tag{30}$$
$$\overline{E}_1(-k_{1z}) = \overline{E}_1(k_{1z}) \tag{31}$$
$$\overline{H}_1(-k_{1z}) = \overline{H}_1(k_{1z}) \tag{32}$$

In addition, another important property is extracted from a close examination of Eqs. (28) and (29), which is the following: the wave number k_1 does not appear in $\overline{\overline{G}}_{00,20}$, and appears as k_1^2 in the Green's function $\overline{\overline{G}}_{10}$. Therefore, the Green's functions in all regions are invariant with respect to the sign of k_1 also. Notice that this conclusion is not surprising since the waves expressed in Eqs. (1)–(3) include waves in all possible directions.

3. CURRENT SOURCE WITH GAUSSIAN DISTRIBUTION

In the previous section, the developments of the Green's functions have been kept very general. In the present section though, we shall particularize the treatment to $\epsilon_1 = -\epsilon_0,\ \mu_1 = -\mu_0$. Hence, the Green's functions given by Eqs. (1)–(3) can now be written as:

$$\begin{aligned}
\overline{\overline{G}}_{00}(\overline{r},\overline{r}') &= \frac{i}{8\pi^2}\iint \mathrm{d}k_x\mathrm{d}k_y \frac{1}{k_{0z}}\Big\{\Big[\hat{e}(-k_{0z})e^{i\overline{K}\cdot\overline{r}}\Big]\,\hat{e}(-k_{0z})e^{-i\overline{K}\cdot\overline{r}'} \\
&\quad + \Big[\hat{h}(-k_{0z})e^{i\overline{K}\cdot\overline{r}}\Big]\,\hat{h}(-k_{0z})e^{-i\overline{K}\cdot\overline{r}'}\Big\} \qquad (33)\\
\overline{\overline{G}}_{10}(\overline{r},\overline{r}') &= \frac{i}{8\pi^2}\iint \mathrm{d}k_x\mathrm{d}k_y \frac{1}{k_{0z}}\Big\{\Big[\hat{e}(k_{0z})e^{i\overline{k}\cdot\overline{r}}\Big]\,\hat{e}(-k_{0z})e^{-i\overline{K}\cdot\overline{r}'} \\
&\quad - \Big[\hat{h}(k_{0z})e^{i\overline{k}\cdot\overline{r}}\Big]\,\hat{h}(-k_{0z})e^{-i\overline{K}\cdot\overline{r}'}\Big\} \qquad (34)\\
\overline{\overline{G}}_{20}(\overline{r},\overline{r}') &= \frac{i}{8\pi^2}\iint \mathrm{d}k_x\mathrm{d}k_y \frac{1}{k_{0z}}e^{-i2k_{0z}d}\Big\{\Big[\hat{e}(-k_{0z})e^{i\overline{K}\cdot\overline{r}}\Big]\hat{e}(-k_{0z})e^{-i\overline{K}\cdot\overline{r}'} \\
&\quad + \Big[\hat{h}(-k_{0z})e^{i\overline{K}\cdot\overline{r}}\Big]\,\hat{h}(-k_{0z})e^{-i\overline{K}\cdot\overline{r}'}\Big\} \qquad (35)
\end{aligned}$$

In addition, we shall also suppose from now on that the current source is placed above the slab at $z = h$, and has a Gaussian distribution in the transverse xy-plane expressed by:

$$\overline{J}(\overline{r}') = \hat{y}I_o\ell\delta(z'-h)\frac{e^{-x'^2/g_x^2+i\beta_x x'}}{\sqrt{\pi}g_x}\,\frac{e^{-y'^2/g_y^2+i\beta_y y'}}{\sqrt{\pi}g_y} \qquad (36)$$

where g_x and g_y are factors specifying the expansion size of the current in the horizontal xy-plane, β_x and β_y are the parameters of phase shift, and $I_o\ell$ is the amplitude of the current distribution with the same units as a dipole moment. For simplicity, we assume here that $\beta_x = \beta_y = 0$. Upon using Eq. (12), the Greeen's functions (33)–(35) and the current distribution (36), we obtain the electric and magnetic fields for the x-, y-, and z-components as listed in Appendix A.3. Particularly, in

the xz-plane where $y = 0$, the expressions for the fields are simplified further to eventually yield:

1. In region 0 ($0 \le z \le h$),

$$E_{0y}(\overline{r}) = -\frac{\omega\mu_0 k}{8\pi^2} I_o \ell I_y(x, z-h) \tag{37}$$

$$E_{0x,0z}(\overline{r}) = -\frac{k^2}{8\pi^2} I_o \ell I_{x,z}(x, z-h) \tag{38}$$

$$E_{0x}(\overline{r}) = E_{0z}(\overline{r}) = H_{0y}(\overline{r}) = 0 \tag{39}$$

2. In region 1 ($-d \le z < 0$),

$$E_{1y}(\overline{r}) = -\frac{\omega\mu_0 k}{8\pi^2} I_o \ell I_y(x, -z-h) \tag{40}$$

$$E_{1x,1z}(\overline{r}) = -\frac{k^2}{8\pi^2} I_o \ell I_{x,z}(x, -z-h) \tag{41}$$

$$E_{1x}(\overline{r}) = E_{1z}(\overline{r}) = H_{1y}(\overline{r}) = 0 \tag{42}$$

3. In region 2 ($z < -d$),

$$E_{2y}(\overline{r}) = -\frac{\omega\mu_0 k}{8\pi^2} I_o \ell I_y(x, z+2d-h) \tag{43}$$

$$E_{2x,2z}(\overline{r}) = -\frac{k^2}{8\pi^2} I_o \ell I_{x,z}(x, z+2d-h) \tag{44}$$

$$E_{2z}(\overline{r}) = E_{2x}(\overline{r}) = H_{2y}(\overline{r}) = 0 \tag{45}$$

where we have defined

$$I_x(x,z) = \int_0^\infty \mathrm{d}s \int_0^{2\pi} \mathrm{d}\phi s\psi(s,\phi) e^{-ik\sqrt{1-s^2}z} e^{iksx\cos\phi} \tag{46}$$

$$I_y(x,z) = \int_0^\infty \mathrm{d}s \int_0^{2\pi} \mathrm{d}\phi s \frac{1-s^2\sin^2\phi}{\sqrt{1-s^2}} \psi(s,\phi) e^{-ik\sqrt{1-s^2}z} e^{iksx\cos\phi} \tag{47}$$

$$I_z(x,z) = \int_0^\infty \mathrm{d}s \int_0^{2\pi} \mathrm{d}\phi \frac{s^2\cos\phi}{\sqrt{1-s^2}} \psi(s,\phi) e^{-ik\sqrt{1-s^2}z} e^{iksx\cos\phi} \tag{48}$$

with $\psi(s,\phi) = e^{-\frac{g_x^2 k^2 s^2 \cos^2\phi}{4}} e^{-\frac{g_y^2 k^2 s^2 \sin^2\phi}{4}}$.

The numerical computation of the fields in the different regions has been performed at a frequency of $f = 30\,\mathrm{GHz}$, with the permittivity and the permeability of the slab set to $-\epsilon_0$, $-\mu_0$, respectively, and a thickness of $d = 8\,\lambda$, or 8 cm (λ being the wavelength in free-space). The current distribution is specified by the factors $g_x = g_y = 1.2\,\lambda$ and $\beta_x = \beta_y = 0$. The units of the field plots are all in $I_o\ell$.

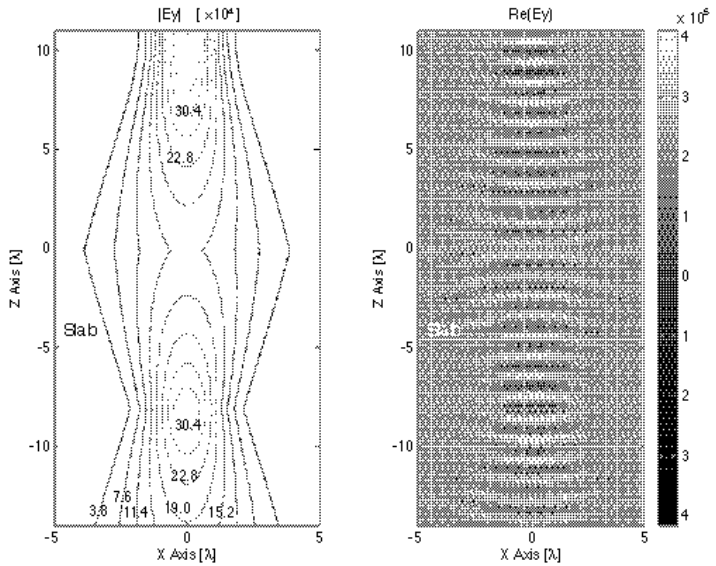

Figure 2. y-component of the electric field propagating through a slab of thickness $d = 8\,\lambda$ ($f = 30\,\text{GHz}$), with constitutive parameters $(-\epsilon_0, -\mu_0)$. The current source is placed at $z = 11\,\lambda$. The units of the field amplitude are $I_o\ell$. Left: $|E_y|$. Right: $\text{Re}(E_y)$.

Fig. 2 shows the contour plot of E_y component for the current source placed at $z = 11\,\lambda$, over the slab, namely at a distance to the first interface superior than the slab thickness. The left plot is the absolute value of E_y, which gives the time-averaged E_y field, whereas the right plot is the real part of E_y, which represents the instantaneous E_y field at time $t = 0$. Notice the continuity of E_y across the boundaries at $z = 0$ and $z = -8\,\lambda$. Figs. 3 and 4 show the x- and z-components of the magnetic field $\overline{H}$, respectively. Note that the tangential component H_x is continuous at the boundaries ($z = 0,\ z = -8\,\lambda$), while the normal component H_z is not, as expected. The Poynting power is shown in Fig. 5, where the left plot is the amplitude of the time-averaged Poynting power overlapped with arrows indicating the direction of the power ow. Note that the direction of the Poynting power flow is consistently in the direction away from the current source. The right plot in Fig. 5 shows the amplitude value of $\text{Re}(\overline{E}) \times \text{Re}(\overline{H})$, which represents the instantaneous Poynting power.

Figs. 6–9 show the fields, E_y, H_x and H_z, and Poynting power flow for a current source placed at $z = 5\,\lambda$, namely at a distance to the first interface inferior than the slab thickness. Note that perfect images for

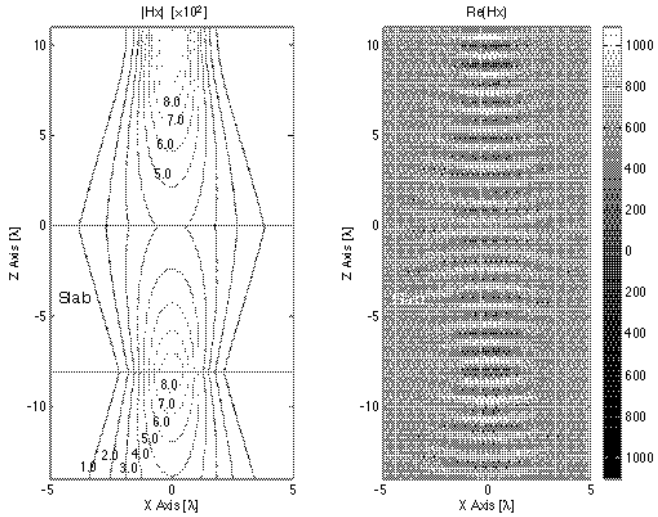

Figure 3. x-component of the magnetic field propagating through a slab of thickness $d = 8\,\lambda$ ($f = 30\,\mathrm{GHz}$), with constitutive parameters $(-\epsilon_0, -\mu_0)$. The current source is placed at $z = 11\,\lambda$. The units of the field amplitude are $I_o\ell$. Left: $|H_x|$. Right: $\mathrm{Re}(H_x)$.

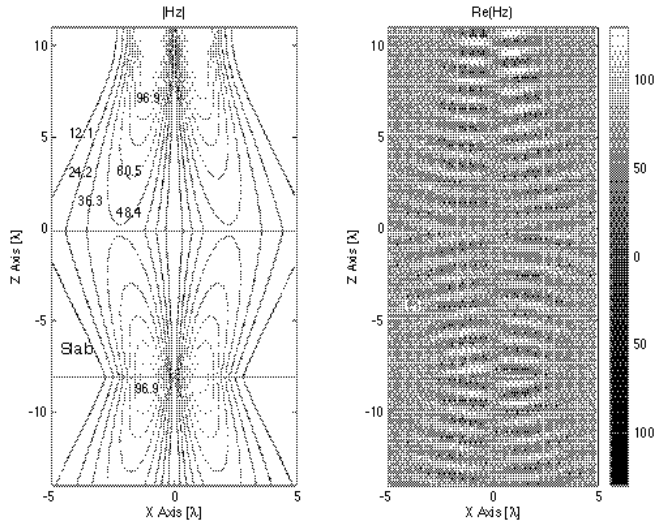

Figure 4. z-component of the magnetic field propagating through a slab of thickness $d = 8\,\lambda$ ($f = 30\,\mathrm{GHz}$), with constitutive parameters $(-\epsilon_0, -\mu_0)$. The current source is placed at $z = 11\,\lambda$. The units of the field amplitude are $I_o\ell$. Left: $|H_z|$. Right: $\mathrm{Re}(H_z)$.

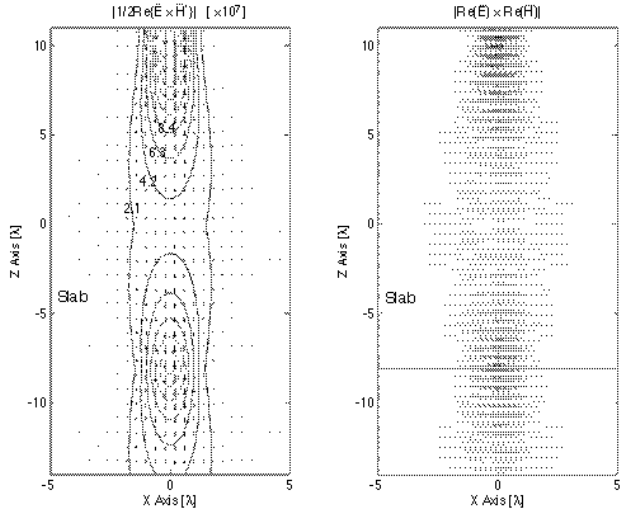

Figure 5. Poynting Power for a slab with $(-\epsilon_0, -\mu_0)$ and thickness $d = 8\,\lambda$ ($f = 30\,\mathrm{GHz}$). The current source is placed at $z = 11\,\lambda$. The units of the field amplitude are $|I_o\ell|^2$. Left: $|\langle\overline{S}\rangle|$ with arrows indicating the directions of power flow, $\langle\rangle$ denoting the time averaging. Right: $|\mathrm{Re}(\overline{E}) \times \mathrm{Re}(\overline{H})|$.

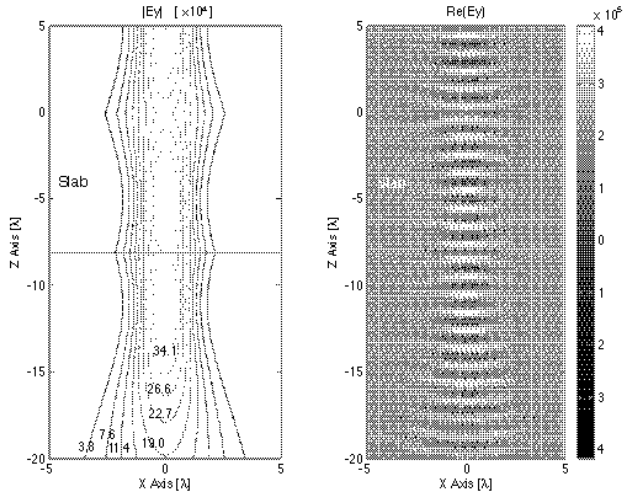

Figure 6. y-component of the electric field propagating through a slab of thickness $d = 8\,\lambda$ ($f = 30\,\mathrm{GHz}$), with constitutive parameters $(-\epsilon_0, -\mu_0)$. The current source is placed at $z = 5\,\lambda$. The units of the field amplitude are $I_o\ell$. Left: $|E_y|$. Right: $\mathrm{Re}(E_y)$.

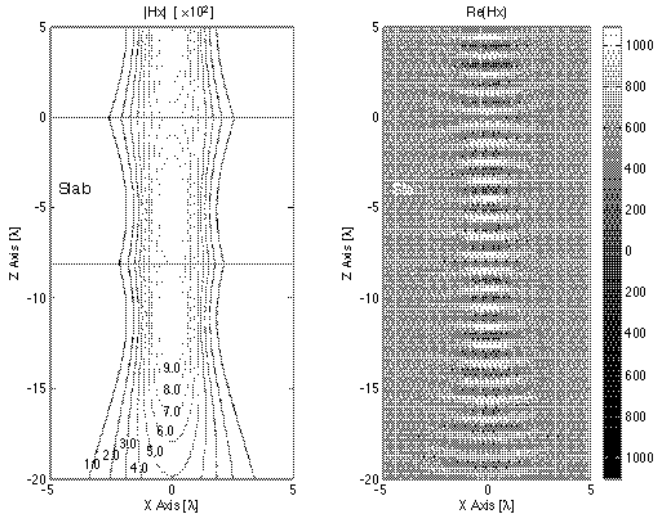

Figure 7. x-component of the magnetic field propagating through a slab of thickness $d = 8\,\lambda$ ($f = 30\,\mathrm{GHz}$), with constitutive parameters $(-\epsilon_0, -\mu_0)$. The current source is placed at $z = 5\,\lambda$. The units of the field amplitude are $I_o\ell$. Left: $|H_x|$. Right: $\mathrm{Re}(H_x)$.

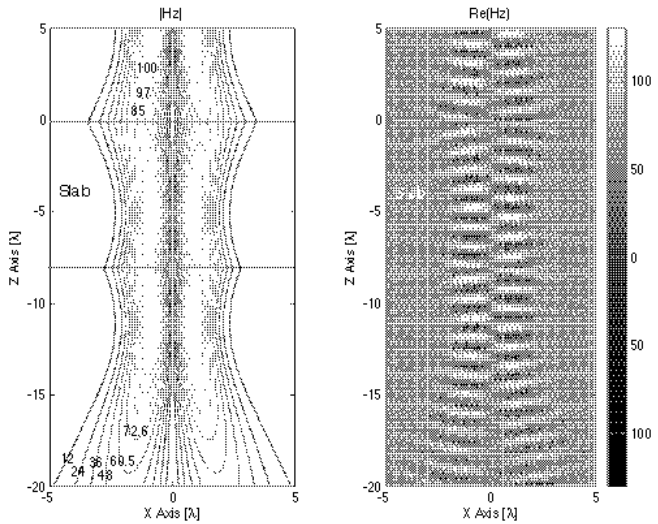

Figure 8. z-component of the magnetic field propagating through a slab of thickness $d = 8\,\lambda$ ($f = 30\,\mathrm{GHz}$), with constitutive parameters $(-\epsilon_0, -\mu_0)$. The current source is placed at $z = 5\,\lambda$. The units of the field amplitude are $I_o\ell$. Left: $|H_z|$. Right: $\mathrm{Re}(H_z)$.

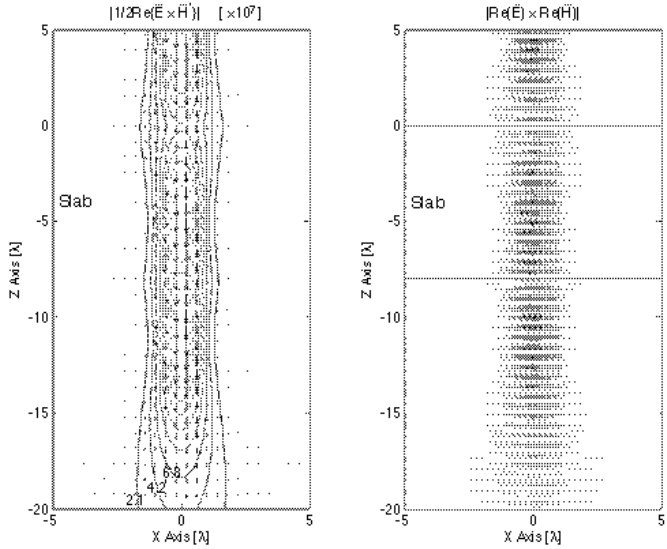

Figure 9. Poynting Power for a slab with $(-\epsilon_0, -\mu_0)$ and thickness $d = 8\,\lambda$. The current source is placed at $z = 5\,\lambda$ ($f = 30\,\text{GHz}$). The units of the field amplitude are $|I_o\ell|^2$. Left: $|\langle\overline{S}\rangle|$ with arrows indicating the directions of power flow, $\langle\rangle$ denoting the time averaging. Right: $|\text{Re}(\overline{E}) \times \text{Re}(\overline{H})|$.

the field at $z = 5\,\lambda$ are formed at $z = -5\,\lambda$ in the slab and $z = -11\,\lambda$ below the slab. In other words, this slab forms identical image fields inside the slab in the region $-8\,\lambda < z < -5\,\lambda$ and outside the slab in the region $z < -11\,\lambda$ to the "source field" in the region $0 < z < 5\,\lambda$. More generally, if the condition $h < d$ is satisfied, two perfect images will be formed, one in each region $0 > z > -d$ and $z < -d$. The exact location of these images has already been predicted in [1, 5] and in our case, can also be directly verified from Eqs. (40)–(45) to be at:

$$z_{\text{image 1}} = -h \tag{49}$$

$$z_{\text{image 2}} = h - 2d \tag{50}$$

4. CONCLUSIONS

Electromagnetic waves inside and outside a slab made of a medium with both ϵ_1 and μ_1 negative have been studied by using the layered Green's function formulations, with coefficients of plane waves determined from the boundary conditions for the tangential electric

and magnetic fields. The layered Green's functions include complete sets of planewave components, and it has been shown that the final solution of the Green's functions and the fields are invariant with respect to the signs of the wave numbers k_1 and k_{1z} in the slab. Consequently, it appears that in general, the up- and down-going waves for propagating waves, and the growing and decaying waves for evanescent waves may all exist inside the slab. For the special case in which the slab has $\epsilon_1 = -\epsilon_0$ and $\mu_1 = -\mu_0$, the evanescent waves in the slab are growing in amplitude and the wave vector has an opposite direction to the direction of the Poynting power ow. Finally, for a slab with $\epsilon_1 = -\epsilon_0$ and $\mu_1 = -\mu_0$ and a current source located at a proper position, the image fields are found inside and outside the slab, and are identical to the field radiated in the source region.

APPENDIX A.

A.1. Boundary Conditions

In the situation of Fig. 1, boundary conditions applied on the electromagnetic field lead to the following system of equations:

For TE Waves:

$$1 + R^{TE} = B + A \tag{A1}$$

$$\frac{k_{0z}}{\mu_0}\left(-1 + R^{TE}\right) = \frac{k_{1z}}{\mu_1}(-B + A) \tag{A2}$$

$$Be^{ik_{1z}d} + Ae^{-ik_{1z}d} = T^{TE}e^{ik_{0z}d} \tag{A3}$$

$$\frac{k_{1z}}{\mu_1}\left(-Be^{ik_{1z}d} + Ae^{-ik_{1z}d}\right) = -\frac{k_{0z}}{\mu_0}T^{TE}e^{ik_{0z}d} \tag{A4}$$

For TM waves:

$$\frac{k_{0z}}{k}\left(1 - R^{TM}\right) = \frac{k_{1z}}{k_1}(D - C) \tag{A5}$$

$$\frac{k}{\mu_0}\left(1 + R^{TM}\right) = \frac{k_1}{\mu_1}(D + C) \tag{A6}$$

$$\frac{k_{1z}}{k_1}\left(De^{ik_{1z}d} - Ce^{-ik_{1z}d}\right) = T^{TM}\frac{k_{0z}}{k}e^{ik_{0z}d} \tag{A7}$$

$$\frac{k_1}{\mu_1}\left(De^{ik_{1z}d} + Ce^{-ik_{1z}d}\right) = \frac{k}{\mu_0}T^{TM}e^{ik_{0z}d} \tag{A8}$$

A.2. Fresnel Reflection Coefficients

$$R_{01}^{TE,TM} = \frac{1 - p_{01}^{TE,TM}}{1 + p_{01}^{TE,TM}} = -R_{10}^{TE,TM} \tag{A9}$$

where

$$p_{01}^{TE} = \frac{\mu_0 k_{1z}}{\mu_1 k_{0z}} = 1 \Big/ p_{10}^{TE} \tag{A10}$$

$$p_{01}^{TM} = \frac{\epsilon_0 k_{1z}}{\epsilon_1 k_{0z}} = 1 \Big/ p_{10}^{TM} \tag{A11}$$

A.3. Electromagnetic Fields for a Slab with $(-\epsilon_0, -\mu_0)$ and a Gaussian Distributed Current Source

In region 0 $(0 \le z \le h)$,

$$E_{0x}(\overline{r}) = \frac{\omega\mu_0}{8\pi^2 k^2} I_o \ell \iint \mathrm{d}k_x \mathrm{d}k_y \frac{k_x k_y}{k_{0z}} e^{ik_x x + ik_y y} \psi(k_x, k_y) \tag{A12}$$

$$E_{0y}(\overline{r}) = -\frac{\omega\mu_0}{8\pi^2 k^2} I_o \ell \iint \mathrm{d}k_x \mathrm{d}k_y \frac{1}{k_{0z}} e^{ik_x x + ik_y y} e^{-ik_{0z}(z-h)} e^{-ik_{0z}(z-h)} \cdot (k^2 - k_y^2) \psi(k_x, k_y) \tag{A13}$$

$$E_{0z}(\overline{r}) = -\frac{\omega\mu_0}{8\pi^2 k^2} I_o \ell \iint \mathrm{d}k_x \mathrm{d}k_y k_y e^{ik_x x + ik_y y} e^{-ik_{0z}(z-h)} \psi(k_x, k_y) \tag{A14}$$

$$H_{0x}(\overline{r}) = -\frac{1}{8\pi^2} I_o \ell \iint \mathrm{d}k_x \mathrm{d}k_y e^{ik_x x + ik_y y} e^{-ik_{0z}(z-h)} \psi(k_x, k_y) \tag{A15}$$

$$H_{0y}(\overline{r}) = 0 \tag{A16}$$

$$H_{0z}(\overline{r}) = -\frac{1}{8\pi^2} I_o \ell \iint \mathrm{d}k_x \mathrm{d}k_y \frac{k_x}{k_{0z}} e^{ik_x x + ik_y y} e^{-ik_{0z}(z-h)} \psi(k_x, k_y) \tag{A17}$$

In region 1 $(-d \le z < 0)$,

$$E_{1x}(\overline{r}) = \frac{\omega\mu_0}{8\pi^2 k^2} I_o \ell \iint \mathrm{d}k_x \mathrm{d}k_y \frac{k_x k_y}{k_{0z}} e^{ik_x x + ik_y y} e^{ik_{0z}(z+h)} \psi(k_x, k_y) \tag{A18}$$

$$E_{1y}(\overline{r}) = -\frac{\omega\mu_0}{8\pi^2 k^2} I_o \ell \iint \mathrm{d}k_x \mathrm{d}k_y \frac{k^2 - k_y^2}{k_{0z}} e^{ik_x x + ik_y y} e^{ik_{0z}(z+h)} \psi(k_x, k_y) \tag{A19}$$

$$E_{1z}(\overline{r}) = \frac{\omega\mu_0}{8\pi^2 k^2} I_o \ell \iint \mathrm{d}k_x \mathrm{d}k_y k_y e^{ik_x x + ik_y y} e^{ik_{0z}(z+h)} \psi(k_x, k_y) \tag{A20}$$

$$H_{1x}(\overline{r}) = -\frac{1}{8\pi^2} I_o \ell \iint \mathrm{d}k_x \mathrm{d}k_y e^{ik_x x + ik_y y} e^{ik_{0z}(z+h)} \psi(k_x, k_y) \tag{A21}$$

$$H_{1y}(\overline{r}) = 0 \tag{A22}$$

$$H_{1z}(\overline{r}) = -\frac{1}{8\pi^2} I_o \ell \iint \mathrm{d}k_x \mathrm{d}k_y \frac{k_x}{k_{0z}} e^{ik_x x + ik_y y} e^{ik_{0z}(z+h)} \psi(k_x, k_y) \tag{A23}$$

In region 2 ($z \leq -d$),

$$E_{2x}(\overline{r}) = \frac{\omega\mu_0}{8\pi^2 k^2} I_o \ell \iint \mathrm{d}k_x \mathrm{d}k_y \frac{k_x k_y}{k_{0z}} e^{ik_x x + ik_y y} e^{-ik_{0z}(z+2d-h)} \psi(k_x, k_y) \tag{A24}$$

$$E_{2y}(\overline{r}) = -\frac{\omega\mu_0}{8\pi^2 k^2} I_o \ell \iint \mathrm{d}k_x \mathrm{d}k_y \frac{1}{k_{0z}} e^{ik_x x + ik_y y} e^{-ik_{0z}(z+2d-h)} \cdot (k^2 - k_y^2)\psi(k_x, k_y) \tag{A25}$$

$$E_{2z}(\overline{r}) = -\frac{\omega\mu_0}{8\pi^2 k^2} I_o \ell \iint \mathrm{d}k_x \mathrm{d}k_y k_y e^{ik_x x + ik_y y} e^{-ik_{0z}(z+2d-h)} \psi(k_x, k_y) \tag{A26}$$

$$H_{2x}(\overline{r}) = -\frac{1}{8\pi^2} I_o \ell \iint \mathrm{d}k_x \mathrm{d}k_y e^{ik_x x + ik_y y} e^{-ik_{0z}(z+2d-h)} \psi(k_x, k_y) \tag{A27}$$

$$H_{2y}(\overline{r}) = 0 \tag{A28}$$

$$H_{2z}(\overline{r}) = -I_o \ell \frac{1}{8\pi^2} \iint \mathrm{d}k_x \mathrm{d}k_y \frac{k_x}{k_{0z}} e^{ik_x x + ik_y y} e^{-ik_{0z}(z+2d-h)} \psi(k_x, k_y) \tag{A29}$$

where

$$\psi(k_x, k_y) = e^{-\frac{g_x^2 (k_x - \beta_x)^2}{4}} e^{-\frac{g_y^2 (k_y - \beta_y)^2}{4}} \tag{A30}$$

REFERENCES

1. Veselago, V. G., "The electrodynamics of substances with simultaneously negative values of ϵ and μ," *Sov. Phys. Usp.,* Vol. 10, No. 4, 509–514, Jan.–Feb. 1968.
2. Pendry, J., A. Holden, W. Stewart, and I. Youngs, "Extremely low frequency plasmons in metallic mesostructures," *Phys. Rev. Lett.,* Vol. 76, 4773–4776, June 1996.
3. Pendry, J., A. Holden, and W. Stewart, "Magnetism from conductors and enhanced nonlinear phenomena," *IEEE Trans. Microwave Theory Tech.,* Vol. 47, No. 18, 2075–2084, Nov. 1999.
4. Smith, D. R., W. J. Padilla, D. C. Vier, S. C. Nemat-Nasser, and S. Schultz, "Composite medium with simultaneously negative permeability and permittivity," *Phys. Rev. Lett.,* Vol. 84, No. 18, 4184–4187, May 2000.
5. Pendry, J. B., "Negative refraction makes a perfect lens," *Phys. Rev. Lett.,* Vol. 85, No. 18, 3966–3969, Oct. 2000.
6. Kong, J. A., *Electromagnetic Wave Theory,* EMW Publishing, Cambridge, Massachusetts, 2000.